



## **Technical Paper**

### **A potential flow model for wind turbine induction and wind farm blockage**

Brian J Gribben and Graham S Hawkes  
Frazer-Nash Consultancy

# A potential flow model for wind turbine induction and wind farm blockage

Brian J Gribben and Graham S Hawkes, Frazer-Nash Consultancy

14 June 2019

---

## ABSTRACT

A simple model based on potential flow theory is introduced for the induction deceleration or blockage effect upwind of a wind turbine. An overall model for the blockage effect of a wind farm can be obtained by combining several representations of wind turbines. An initial comparison with results from a vortex cylinder model shows good agreement. The model may be applied in combination with wake effects methods to correct wind resource assessment results for blockage effects. Further validation with measured wind speed data would be required to establish the predictive power of the model.

## INTRODUCTION

In the induction zone, a wind turbine slows down the upwind flow ahead of the rotor. Conventional wind resource assessment methods do not take account of this wind turbine scale effect possibly accumulating to a wind farm scale. Evidence for the presence of appreciable wind farm blockage effects has developed and there is a concern that the potential impact on wind farm energy yield is neither understood nor quantified.

An estimate of the upwind deceleration for a single wind turbine is provided by the vortex cylinder model,<sup>1,2</sup> which is often used in axial centre-line expression form.<sup>3,4</sup> This predicts, 2.5 rotor diameters upwind of the rotor disk, a wind speed reduction from the notional freestream/undisturbed value of roughly 0.5% for common thrust coefficient magnitudes below rated power. There is scope to expand the validation basis of the model, but that it is realistic and useful is supported by various studies comparing with measurement,<sup>5</sup> wind tunnel and computational fluid dynamics<sup>3</sup> results. Here this model is considered as a lower bound on a turbine's induction deceleration; a lower bound because the model does not represent ground effect, and is essentially inviscid, and interaction with the boundary layer is likely to increase rather than diminish the magnitude of induction effects.

Wind speed measurements at Alpha Ventus indicate an upwind deceleration in the range 1% to 2% of undisturbed inflow wind speed.<sup>6</sup> Inflow wind speeds from a number of other offshore wind farms have been fitted to an induction model, also indicating an upwind deceleration greater than might be anticipated from a single turbine.<sup>7</sup> In combination with reports of non-negligible variation in power generated by windward turbines at offshore wind farms of 10% and beyond<sup>8,9</sup> this indicates that a wind farm's blockage effect may be significant. In an onshore context, a computational fluid dynamics model has been

applied to wind farm blockage with some good agreement to measured wind speed data, before and after wind farm construction.<sup>10</sup>

There is not yet a simple engineering model for wind farm blockage, nor does there exist a robust validation against measured data which establishes trust in the predictive power of models. The focus of this communication is the former, namely to derive a simple engineering model for wind farm blockage effects, with a particular emphasis on offshore wind farms.

### **RANKINE HALF BODY**

From potential flow theory,<sup>11</sup> combining a source with a uniform flow results in a flow pattern with velocity components (in a spherical coordinate system  $(r, \theta)$ , with the source located at  $r = 0$ ) as follows:

$$v_r = \frac{m}{4\pi r^2} + U \cos \theta$$

$$v_\theta = -U \sin \theta$$

The stagnation streamline describes a body of revolution known as a Rankine Half Body (RHB):

$$\cos \theta - \frac{2\pi U}{m} r^2 \sin^2 \theta = -1$$

In the above,  $m$  is the source strength and  $U$  is a uniform flow along the direction  $\theta = 0$ ; the circumferential coordinate is not present as the flow is invariant circumferentially. In Cartesian coordinates  $(x, y, z)$ , with the source located at  $(0,0,0)$ , the respective velocity components  $(u, v, w)$  are:

$$u = \frac{m}{4\pi} \frac{x}{(x^2 + y^2 + z^2)^{3/2}} + U$$

$$v = \frac{m}{4\pi} \frac{y}{(x^2 + y^2 + z^2)^{3/2}}$$

$$w = \frac{m}{4\pi} \frac{z}{(x^2 + y^2 + z^2)^{3/2}}$$

The Cartesian and spherical coordinate systems are indicated in Figure 1.

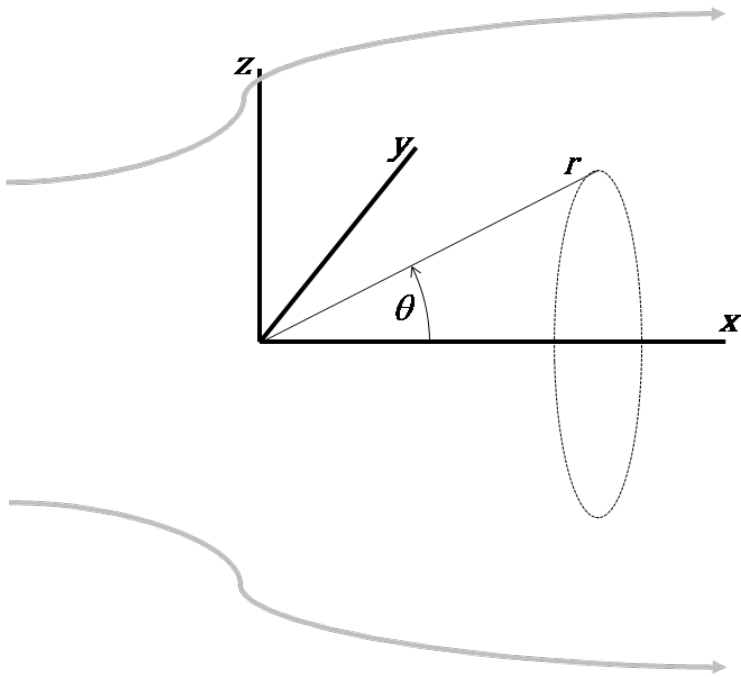


Figure 1: Axisymmetric flow with spherical coordinates, after Shames<sup>11</sup>.

At large  $r$  it can be shown<sup>11</sup> that the maximum cross sectional area  $A_{max}$  of the body of revolution is related to the source strength and the uniform wind speed as follows:

$$m = UA_{max} \quad (1)$$

Similarly, it can be shown that the cross-sectional area at the origin  $A_0$  is related to the maximum cross-sectional area:

$$A_0 = \frac{1}{2}A_{max} \quad (2)$$

### STREAMTUBE MATCHING

The flow field upwind of and around a RHB is shown in Figure 2, Figure 3 and Figure 4.



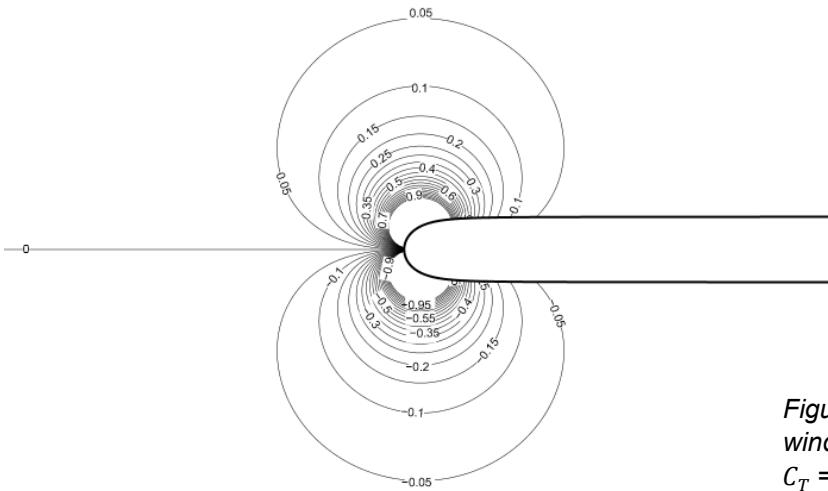


Figure 4: Contours of cross-stream wind speed around RHB,  $U = 10$  m/s,  $C_T = 0.85$ , and wind coming directly from the left. Contour lines outside the range  $[-1, \dots, 1]$  are excluded for clarity.

This flow field has features which resemble a rotor disc's flow field computed from computational fluid dynamics (CFD) and from vortex cylinder methods<sup>12-14</sup> as follows:

- Wind speed deceleration upwind of the body/disc.
- Wind speed acceleration to the side of and slightly behind the body/disc.
- In the plane of the rotor disc, the axial velocity is the main component, with other components zero or small.

A suitably-sized RHB may therefore be a useful simple model for approximating the upwind and lateral pressure/velocity disturbance caused by the presence of a rotor disc. We can attempt to obtain a suitable approximation for the RHB size by using a continuity argument.

From axial momentum theory (see for example Wilson et al<sup>15</sup>) the flow through a rotor disc can be approximated as

$$u = U(1 - a) \quad (3)$$

where  $a$  is the axial induction factor at the rotor, commonly estimated from the thrust coefficient  $C_T$  as

$$a = \frac{1}{2}(1 - \sqrt{1 - C_T})$$

Therefore the mass flow through the stream tube enclosing the rotor disk of area  $A_{Rotor}$  is

$$uA_{Rotor} = U(1 - a)A_{Rotor}$$

At the rotor disk, to achieve the same mass flow through a stream tube of the same area for an RHB flow requires equating the above mass flow to that flowing through an annulus around the RHB, with an axial velocity equivalent to the free stream velocity:

$$uA_{Rotor} = U(A_{Rotor} - A_0) \quad (4)$$

Matching the stream tube for an actuator disc with that for the flow around a RHB in this way is illustrated in Figure 5.

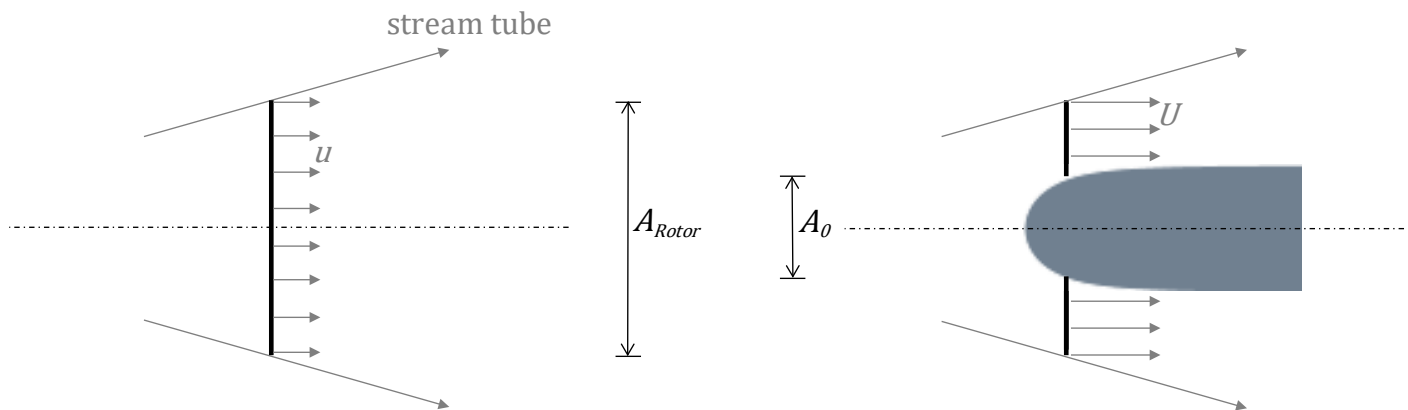


Figure 5: Sizing the RHB flow to approximate the flow ahead of and around an actuator disc (left) by matching the mass flow around an RHB (right) through a stream tube of equivalent area.

By combining Equation 4 with Equation 3 it can be shown that the cross-sectional area of the RHB is related to the area of the rotor and the induction parameter:

$$A_0 = aA_{Rotor}$$

Finally by combining with Equations 1 and 2 we can relate the source strength to the freestream wind speed, induction parameter, and rotor area:

$$m = 2UaA_{Rotor}$$

We now have a very simple means to estimate the wind speed upwind of and to the side of a wind turbine. Since the model is a linear potential flow model, RHB turbine representations can be combined to (a) model induction effects for wind farms, and (b) apply the “method of images” to account for the proximity of the wind turbine to the ground or sea surface.

### Induction model for single turbine

Figure 2 shows velocity contours from the RHB model for a single turbine case, with the axial and cross-stream components shown in Figures 3 and 4. The effect of flow constriction between the wind turbine and the ground or sea surface can be approximated using the method of images. This is accomplished by introducing a second RHB model of equivalent strength, with a vertical separation equal to double the hub height value. The perturbations to the undisturbed flow field are added linearly. Figure 6 shows resulting velocity contours on a horizontal plane through the hub height (assumed

to be at 80m in this case, with a rotor diameter of 100m), which on close inspection indicates an increased wind speed perturbation compare to Figure 2.

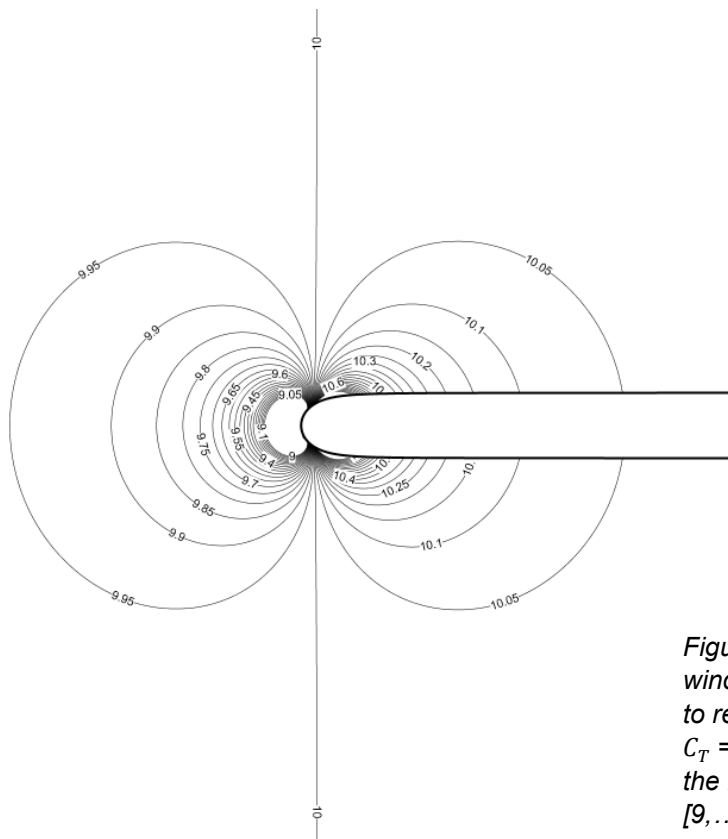


Figure 6: Contours in horizontal plane of wind speed around RHB with image RHB to represent ground effect,  $U = 10$  m/s,  $C_T = 0.85$ , and wind coming directly from the left. Contour lines outside the range [9, ..., 11] are excluded for clarity.

Figure 7 indicates the small upward velocity components in this case.

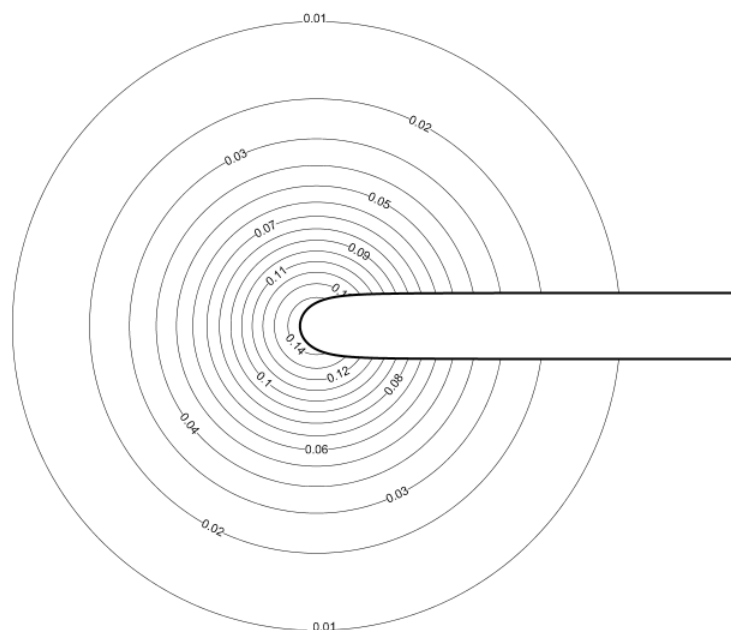


Figure 7: Contours of vertical component of wind speed (out of the page), in the horizontal plane, around RHB with image RHB to represent ground effect,  $U = 10$  m/s,  $C_T = 0.85$ , and wind coming directly from the left.

## Model of induction / blockage for wind farm

Multiple turbine representations can be combined to produce an induction or blockage model for an entire wind farm. Figures 8 and 9 show some modelled results produced in this way – for each a turbine rotor disk of 100m, a hub height of 80 metres and a thrust coefficient of 0.85 was modelled.

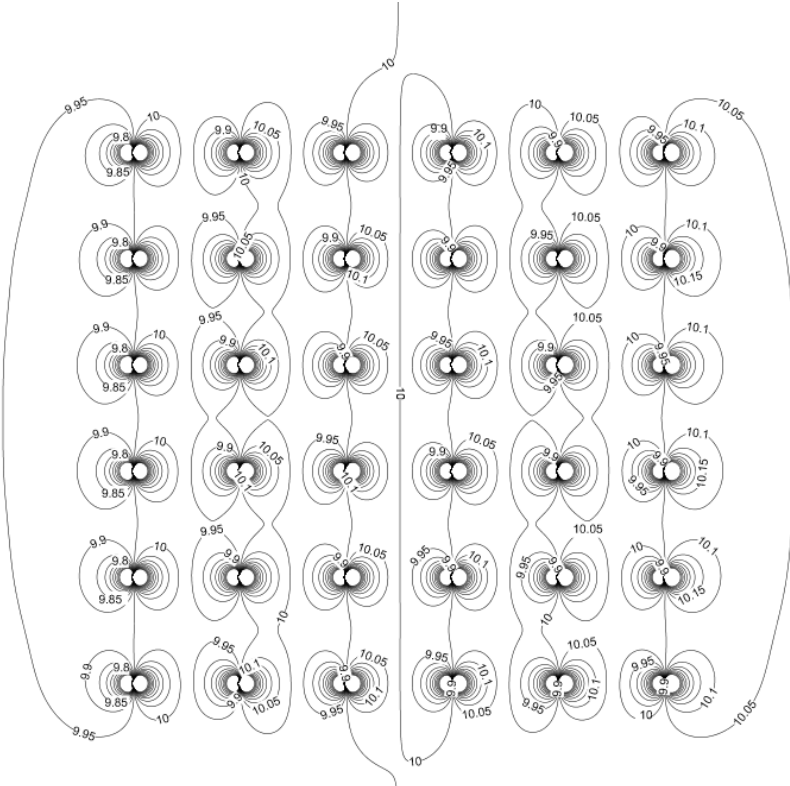


Figure 8: Contours of wind speed perturbation in a wind farm from potential flow model,  $U = 10$  m/s,  $C_T = 0.85$ , and wind coming directly from the left i.e. from 270 degrees. Contour lines outside the range [9, ..., 11] are excluded for clarity. A minimum distance of 7 diameters separates the wind turbine centre-lines. Hub height is at 80m.

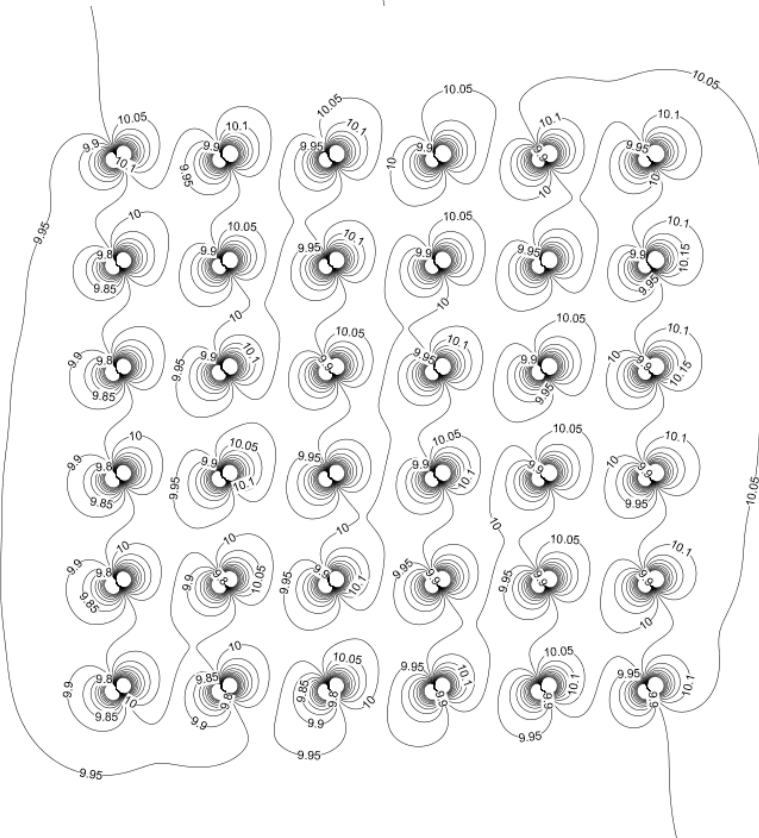


Figure 9: Contours of wind speed perturbation in a wind farm from potential flow model,  $U = 10$  m/s,  $C_T = 0.85$ , and wind coming from 240 degrees. Contour lines outside the range [9, ..., 11] are excluded for clarity. A minimum distance of 7 diameters separates the wind turbine centre-lines. Hub height is at 80m.

The further reduced wind speed from the combined action of the turbine blockage is clearly seen, with the blockage effect increasing for lower hub height and more closely placed turbines, see Figure 10.

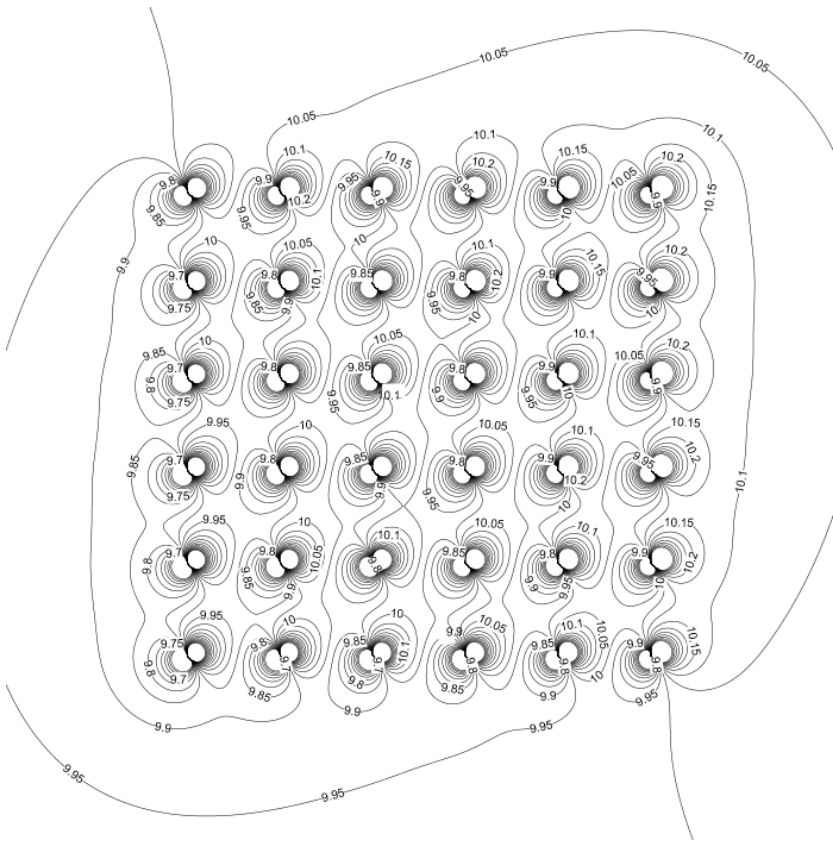


Figure 10: Contours of wind speed perturbation in a wind farm from potential flow model,  $U = 10$  m/s,  $C_T = 0.85$ , and wind coming from 240 degrees. Contour lines outside the range [9, ..., 11] are excluded for clarity. A minimum distance of 5 diameters separates the wind turbine centre-lines. Hub height is at 70m.

### Comparison to vortex cylinder model

Figure 11 shows a comparison of the present RHB model with results from a vortex cylinder model.

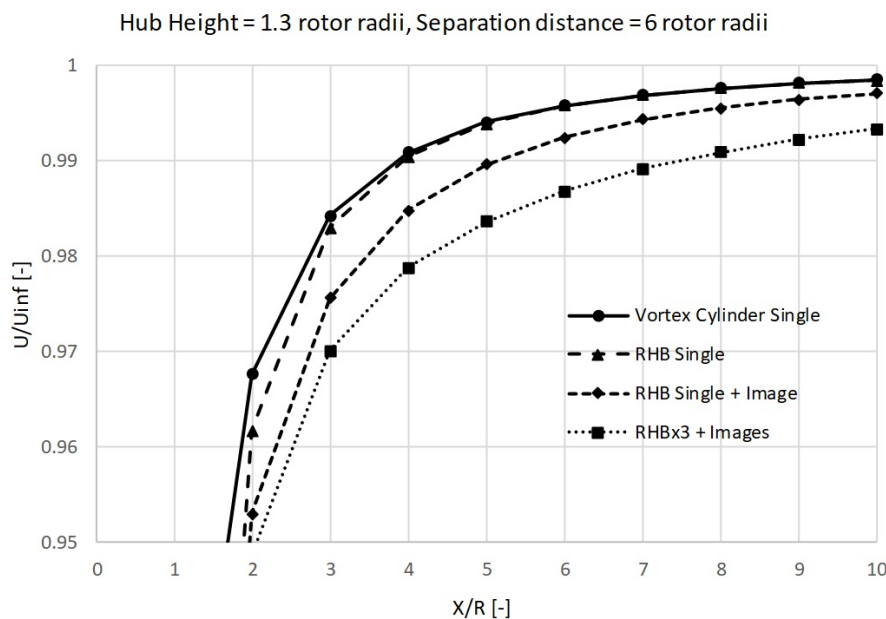


Figure 11: Centre-line induction decelerations predicted by the RHB model.

A thrust coefficient of 0.85 was applied. The flow deceleration on the centreline upwind of a turbine predicted by a single RHB model ('RHB Single') is compared with the equivalent result for a vortex cylinder model ('Vortex Cylinder Simple'). Except for locations close to the turbine, there is a good match; for all credible values of thrust coefficient there is an excellent match on the centreline from 5 times the rotor radius upstream and further upstream.

Also shown are results for an RHB model of a turbine with an added image turbine ('RHB Single + Image') and for RHB models of 3 turbines arranged in a row facing (normal to) the wind, also including images for those turbines ('RHBx3 + Images'). By inspection this appear to match closely a set of similar numerical experiments using the vortex cylinder model which have been previously reported.<sup>7</sup>

## Conclusions

A very simple potential flow model has been introduced which represents the induction effect upwind of and to the side of a wind turbine. It is possible to combine models of turbines to model the overall induction effect of a wind farm.

An initial and very limited comparison of model predictions with those from a vortex cylinder method shows a close agreement. A potential application, in a single turbine context, is in correcting the measured wind speed to produce lower-uncertainty power performance assessments. A second application, in a wind farm context, is in supplementing wake effects calculations with blockage effects corrections.

It should be kept in mind that both vortex cylinder and RHB potential flow models do not in themselves represent interaction with the planetary boundary layer, and have not been the subject of extensive validation work to establish confidence in predictive power, so it remains to be seen whether such an inviscid approach will represent wind turbine induction effects or global blockage effects sufficiently well.

## References

1. Branlard E, Forsting ARM. Using a cylindrical vortex model to assess the induction zone in front of aligned and yawed rotors. In *Proceedings of EWEA Offshore 2015 Conference*, Copenhagen, Denmark, 2015.
2. Branlard E. *Analysis of wind turbine aerodynamics and aeroelasticity using vortex-based methods*. Technical University of Denmark, PhD Thesis, April 2015.
3. Medici D, Ivanelli S, Dahlberg JÅ, Alfredsson PH. The upstream flow of a wind turbine: blockage effect. *Wind Energy* 2011; **14**:691-697.
4. Trolborg N, Meyer Forsting AR. A simple model of the wind turbine induction zone derived from numerical simulations. *Wind Energy* 2017; **20**:2011-2020.
5. Simley E, Angelou N, Mikkelsen T, Sjöholm M, Mann J, Pao LY. Characterization of wind velocities in the upstream induction zone of a wind turbine using scanning continuous-wave LiDARs. *Journal of Renewable and Sustainable Energy* 2016 **8**:013301.
6. Asimakopoulos M, Clive P, More G, Boddington R. Offshore Compression zone measurement and visualisation. *Conference Proceedings EWEA Annual Event*, Barcelona, Spain, 2014.

7. Nygaard NG, Brink FE. Measurements of the wind turbine induction zone: Results from 8 offshore measurement campaigns. Wind Energy Science Conference 2017.
8. Mitraszewski K, Hansen KS, Nygaard NG, Réthoré PE. Wall Effects in Offshore Wind Farms. *European Wind Energy Conference and Exhibition EWEC 2013*. **3**:1349-1358.
9. Iliev S. Array Losses and Array Benefits, The Atmospheric Blockage Effect at Offshore Wind Parks. TU Delft MSc Thesis, April 2014.
10. Bleeg J, Purcell M, Ruisi R, traiger E. Wind Farm Blockage and the Consequences of Neglecting Its Impact on Energy Production. *Energies* 2018, **11**:1609.
11. Shames, IS. *Mechanics of Fluids*. 2<sup>nd</sup> ed. New York, NY: McGraw-Hill; 1982.
12. Meyer Forsting AR, Trolborg N. The effect of blockage on power production for laterally aligned wind turbines. *J. Phys.: Conf. Ser.* **625**:012029 (2015).
13. Meyer Forsting AR, Bechmann A, Trolborg N. A numerical study on the flow upstream of a wind turbine in complex terrain. *J. Phys.: Conf. Ser.* **753**:032041 (2016).
14. Meyer Forsting AR. Modelling Wind Turbine Inflow: The Induction Zone. DTU PhD Thesis, 2017.
15. Wilson RE, Lissaman PBS, Walker SN. *Aerodynamic Performance of Wind Turbines*. Oregon State University, Corvallis, June 1976.

